

Originally published in *Proceedings of the Fifth International Workshop on Compressible Turbulent Mixing*, ed. R. Young, J. Glimm & B. Boston. ISBN 9810229100, World Scientific (1996).

Reproduced with the permission of the publisher.

The Study of the Richtmyer–Meshkov Instability on the Passage of Incident and Reflected Shock Waves through a Gaseous Interface*

S. G. Zaytsev¹, E. I. Chebotareva¹,
A. N. Aleshin¹, E. V. Lazareva¹, S. N. Titov¹,
J. -F. Haas² and M. Le Piouffle²

¹ The Krzhizhanovsky Power Engineering
Institute
Leninsky Pr.19, Moscow, 117071 Russia

² Commissariat à l'Énergie Atomique
Vaujours-Moronvilliers
BP7, 77181 Courtry, France

Abstract. We have made an experimental investigation of the evolution of the Richtmyer-Meshkov Instability (RMI) on the passage of the incident and reflected shock waves through an interface. The experiments have been performed in a shock tube for continuous and discontinuous interfaces. The discontinuous interface was modeled by a thin film. The continuous interface was obtained in a test section with a fast removable plate. We used different combinations of rare gases. One experiment with discontinuous interface has been simulated with a 2D Eulerian code and the agreement is good. We evaluate the dependence of the growth rate of the RMI after reflected shock on the one after incident shock.

1 Introduction

The evolution of the mixing zone between the gases of different density on the passage of a plane shock wave through the sinusoidal interface modeled by a thin film has been studied in [1]. It has been shown that the evolution of the interface separating the shock-compressed gases of different density depends upon the type of refraction of the shock. The type of refraction is determined by the following parameters: $a_0 k$, where a_0 and k are the amplitude and the wave number of initial interface, respectively, the Mach number M of the incident shock wave, and the Atwood number $A = (\rho_2 - \rho_1)(\rho_2 + \rho_1)^{-1}$,

*Partly supported by the Russian Foundation for Fundamental Research (grant no.94-01-01144a), by a contract from the French Atomic Energy Commission (CEA/DAM no.3672), and by the ISTC grant no.94-029.

where ρ_1 and ρ_2 are the densities of gases separated by the interface. Three typical regimes have been described: soft regular, hard regular, and irregular. For the soft regular regime the growth of the amplitude a_{K12} of the initial interface K_{12} at initial stage of the evolution for $\rho_1 < \rho_2$ is satisfactorily described by the Richtmyer relation:

$$\frac{da_{K12}}{dt} = a_{K12}^* ukA \quad (1)$$

where a_{K12}^* is the amplitude at the end of refraction, u the shock-induced velocity of the K_{12} , and A is the Atwood number. For $M = 3$, the relation (1) for the initial stage of the K_{12} evolution is applicable for $a_0k < 2$.

The study of the K_{12} evolution for the shock passage through continuous interface has been made in [2]. It has been shown that for $a_0k < 2$ the growth of the amplitude a_{K12} at the initial stage of the K_{12} evolution is described by the relation (suggested in [3]) within a 30% error:

$$\frac{da_{K12}}{dt} = \frac{a_{K12}^* ukA}{\Psi} \quad (2)$$

The factor Ψ depends on the thickness Δ of interface, wave number k , and Atwood number A and was calculated as described in [4]. To estimate the amplitude a_{K23} of the interface K_{23} formed after the interaction of the reflected shock wave S_{e2b} with K_{12} , one has the choice between adapting relation (2), thus neglecting the influence of the growth rate of a_{K12} :

$$\frac{da_{K23}}{dt} = \frac{a_{K23}^* ukA}{\Psi} \quad (3)$$

or keeping this influence as proposed in [3]:

$$\frac{da_{K23}}{dt} = \frac{da_{K12}}{dt} + \frac{a_{K23}^* ukA}{\Psi(k, \Delta, A)} \quad (4)$$

where a_{K23}^* is the a_{K23} amplitude at the end of refraction of S_{e2b} on K_{12} . The experiments made in [3] allowed the authors to conclude that the relation (4) adequately takes into account the influence of the K_{12} evolution on the K_{23} evolution.

2 Experiments

We performed an experimental and numerical investigation of the passage of the reflected shock wave S_{e2b} through the interface K_{23} . The K_{12} is formed after the passage of the incident shock wave S_{e1a} through the initial interface K_0 . The S_{e1a} propagates in a heavy gas of initial density ρ_1 . The reflected shock wave S_{e2b} propagates in a lighter gas of density ρ_2 . In the first series of experiments made in the shock tube described in [1], the initial discontinuous interface K_0 was modeled by a thin film of sinusoidal shape. The mechanical effect of the shock and the heat effect of the shock-compressed

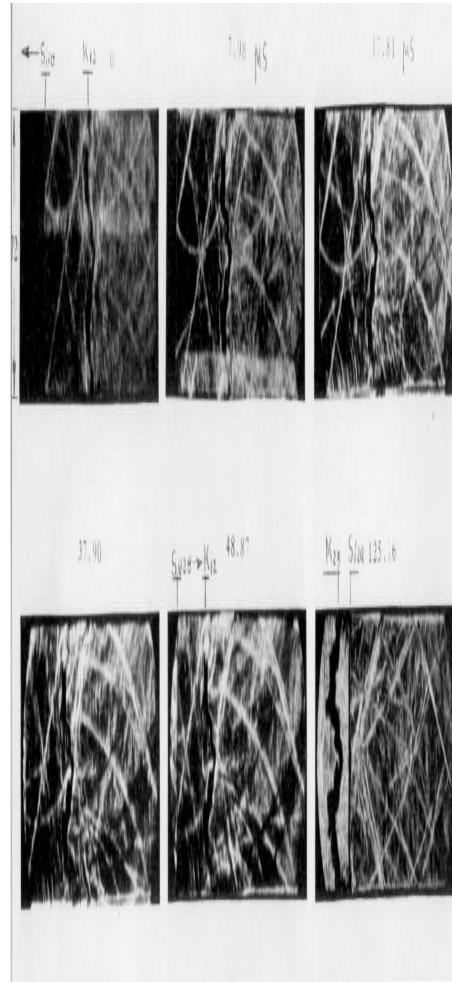


Figure 1: Schlieren pictures of the passage of the incident shock S_{e1a} from Xe to Kr and of the reflected shock S_{e2b} from Kr to Xe (run 583). Times for the figures are (from left to right) 0, 7.98, 17.81 μ s on the top, and 37.90, 48.87, 125.76 μ s on the bottom.

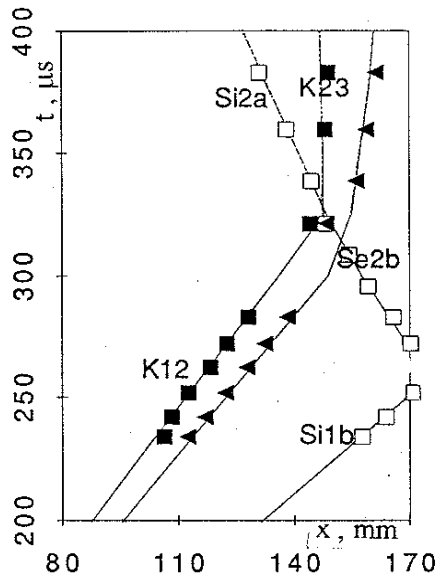


Figure 2: An $x - t$ diagram from run 583, a discontinuous interface with lines from the simulation.

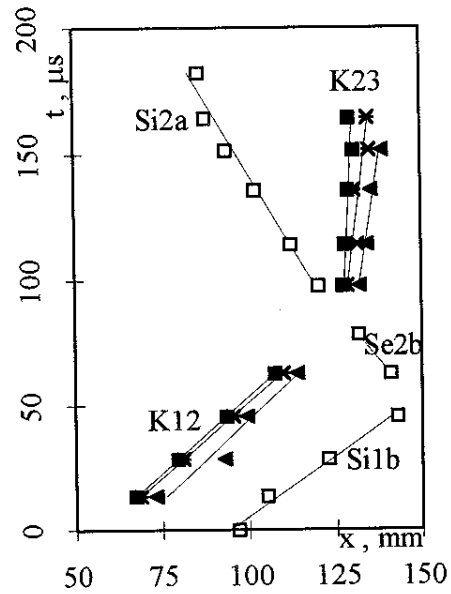


Figure 3: An $x - t$ diagram from run 491, a continuous interface.

flows behind the refracted shock wave S_{i1b} resulted in formation of the mixing zone K_{12} . The K_{12} of sinusoidal shape and finite thickness Δ contained the initial gases and the products of destruction of the film. The refracted shock wave S_{i1b} , reflecting from the end wall of the shock tube, generated the reflected shock wave S_{e2b} which moved toward K_{12} and refracted on it, thus forming the mixing zone K_{23} . In the second series of experiments we used a continuous interface obtained with a fast removable plate separating the gases before the experiment [2]. In this case the distribution of concentrations was dependent on molecular diffusion.

Fig 1 shows the Schlieren pictures for the K_{23} evolution (run 583). The incident shock wave propagated from Xe (right) to Kr (left). The data on K_0 , Mach number of the incident shock wave, and gas combinations are given in table 1. Fig. 2 is the $x - t$ diagram of this experiment with the lines from the simulation (fig. 5). The points for K_{12} and K_{23} are the positions of the experimental crests and troughs of the front separating the mixing zone from the heavy gas (Xe), from which the amplitudes $a_{K12}(t)$ and $a_{23}(t)$ are obtained. S_{i1b} and S_{i2a} are the trajectories of the refracted shock waves generated by the interactions of S_{e1a} with K_0 and of S_{e2b} with K_{12} , respectively. Fig. 4 shows an interferogram of the K_{12} and K_{23} evolutions for the continuous interface (run

experiment	583 disc.	491 cont.	560 disc.	488 cont.
gas 1/gas 2	Xe/Kr	Ar/ $\frac{1}{2}$ Ar+ $\frac{1}{2}$ He	Ar/He	Ar/He
P_0 , bar	0.5	0.5	0.5	0.5
Mach	3.76	3.22	3.74	3.21
λ , mm	36	11.24	72	4.6
a_0 , mm	10		5	
$\frac{da_{K12}}{dt}$, $\frac{mm}{\mu s}$	0.042	0.017	0.092	0.064
$\frac{da_{K23}}{dt}$, $\frac{mm}{\mu s}$	0.077	0.067	0.284	0.207
a_{K23}^* ukA	0.114	0.106	1.017	0.632
$a_{K12}(t_{\mathbf{R}})k$	2.02	1.17	1.49	2.03
$\mathbf{A}_{reshock}$	0.18	0.23	0.76	0.76
refraction	soft	soft	hard	hard
Δ , mm	5.24	3.56	3.08	6.46
χ_1	0.82	0.60	2.98	1.94
χ_2	1.36	0.85	3.30	2.25
Ψ	1.8	2.62	1.2	1.57

Table 1: Initial conditions and results of the experiments.

491). The incident shock wave propagated from Ar (right) to $\frac{1}{2}$ Ar+ $\frac{1}{2}$ He (left). The $x - t$ diagram of this experiment is given in fig. 3 in which the lines are a fit of the experimental points. The 2 extreme lines for K_{12} and K_{23} are the trajectories of the crests on both sides and the intermediate line corresponds to the through on the light gas side ($\frac{1}{2}$ Ar+ $\frac{1}{2}$ He).

The initial conditions and the measured data on the K_{12} and K_{23} evolutions are given in table 1. χ_1 and χ_2 are the ratios of the growth rates calculated from (3) and (4) to the experimentally measured values for $\frac{da_{K12}}{dt}$ and $\frac{da_{K23}}{dt}$. The values of a_{K23}^* were determined from the trajectories of the $K_{12}^{(1)}$, $K_{12}^{(2)}$, $K_{23}^{(1)}$, and $K_{23}^{(2)}$. For the $\Psi(k, \Delta, A)$ we used the values calculated by the method suggested in [4] (Δ is the measured thickness).

3 Numerical simulation

The calculation is based on shock tube experiment 583 with a $M = 3.76$ shock wave refracting on a xenon/krypton discontinuous interface with a 2D single-mode perturbation. We simulate only one wavelength (36 mm). Initial densities and specific heat ratios are respectively 2.655 kg/m³ and 1.645 for xenon and 1.713 kg/m³ and 1.676 for

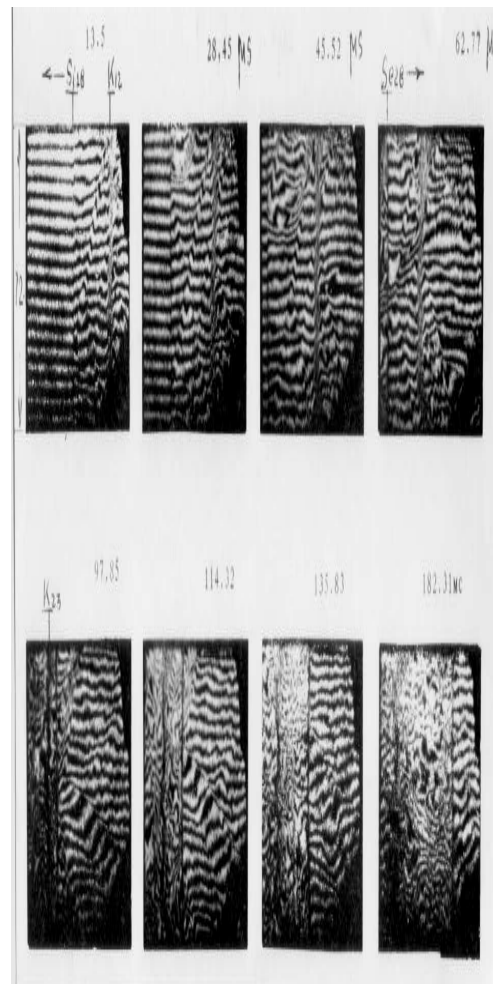


Figure 4: Interferograms of the passage of the incident shock S_{e1a} from Ar to $\frac{1}{2}\text{Ar} + \frac{1}{2}\text{He}$ and of the reflected shock S_{e2b} from $\frac{1}{2}\text{Ar} + \frac{1}{2}\text{He}$ to Ar (run 491). Times are (from left to right) 13.5, 28.45, 45.52, 62.77 μs on the top, and 97.85, 114.32, 135.83, 182.31 μs on the bottom.

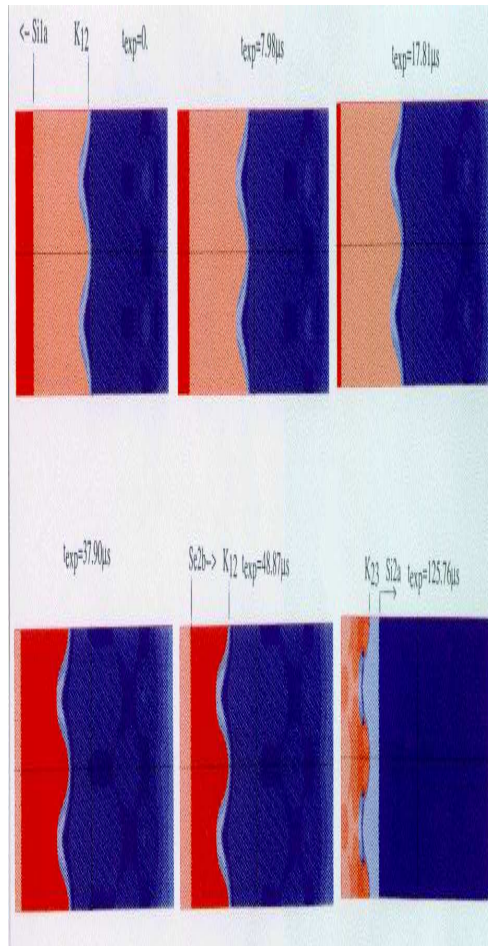


Figure 5: Density maps from the simulation of run 583.

krypton. The code uses 2D Euler compressible and unsteady equations. The initialization uses a Lagrangian step, the Lagrangian grid is then projected on the Eulerian fixed grid. There is no concentration equation, the interfaces between materials are numerically located thanks to the partial volume fraction in "mixed" cells [5]. The BBC finite differences scheme used here is second order in time and fully explicit [6]. The code runs on a Cray YMP computer. With 670 and 100 cells in the streamwise and transverse directions, the interface motion in the region of interest is well refined. Our numerical results illustrated on fig. 2 agree with the experimental data and with theoretical pressures, velocities, densities and sound speeds in each region of the $x - t$ diagram (fig. 5).

4 Conclusion

The results of the study [1] allow us to determine the regime of refraction of S_{e2b} on K_{12} from the experimentally measured interface amplitude $a_{K_{12}}(t_R)$ before interaction of K_{12} with S_{e2b} . It should be considered as a soft regular for the runs 583 and 491, and as a hard regular for the runs 560 and 488. For the soft regime, χ_1 and χ_2 are close to 1 but we cannot discriminate between the relations (3) and (4) as (3) seems more adequate for run 583 and (4) for run 491. For the hard regular regime however, χ_1 and χ_2 are significantly larger than 1 with $\chi_2 > \chi_1$ indicating that relation (4) is less adequate than relation (3). This contrast indicates that the character of the evolution of the mixing zone is dependent on the type of refraction undergone by the reflected shock. Note that χ_1 and χ_2 are lower for continuous interfaces than for the discontinuous ones. Therefore, the question of adequacy of relations (3) and (4), respectively excluding and including the influence of the evolution of K_{12} on the evolution of K_{23} , cannot be settled with these experiments. Solving this problem requires a series of dedicated simulations.

References

- [1] Aleshin A. N., Zaytsev S. G., and Lazareva E. V. (1993), Experimental and numerical studies on Richtmyer-Meshkov Instability. *RJCM*, V. 1, No. 2, p.33-49.
- [2] Zaytsev S. G., Titov S. N., and Chebotareva E. I. (1994), The shock-induced evolution of continuous interface separating gases of different densities. *Izv. Ross. Akad. Nauk. Mekh. Zhidk. i Gaza*, No. 2, p. 18-26.
- [3] Brouillette M. and Sturtevant B. (1994), Experiments on the Richtmyer-Meshkov instability: single-scale perturbation on a continuous interface. *J. Fluid. Mech.*, V. 263, p. 271-292.
- [4] Duff R. E., Harlow F. N., and Hirt S. W. (1962), Effects of diffusion on interface instability between gases. *Phys. Fluids*, V. 5, p. 417-425.
- [5] Youngs D. (1982), Time dependent multi-material flow with large fluid distortion, in *Numerical Methods for Fluid Dynamics*, Morton and Baines eds., Academic Press.

- [6] Sutcliffe W. G. (1973), BBC hydrodynamics. Lawrence Livermore National Laboratory report UCID 17013.